# INHERENT OPTICAL PROPERTIES OF THE AEROSOLS FOR OLCI/SENTINEL-3
# - FROM MICRO-PHYSICAL PROPERTIES TO OPTICAL PROPERTIES USING AERONET -


Richard Santer (1,4), Francis Zagolski (1,2), and Ouahid Aznay (1,3)

(1) ADRINORD, Association pour le Développement de la Recherche et de l'Innovation dans le bassin du Nord-Pas-de-Calais, 2 rue des Cannoniers, F59000, Lille – FRANCE.
E-mail: Santer.Richard@yahoo.fr

(2) PARBLEU Technologies Inc., 79 Veilleux street, St Jean-sur-Richelieu (QC), J3B-3W7 – CANADA.
E-mail: Francis_Zagolski@yahoo.ca

(3) C-S Systèmes d'Information, ZAC de la Grande Plaine, F31506, Toulouse – FRANCE.
E-mail: Ouahid.Aznay@c-s.fr

(4) Université du Littoral Côte d'Opale, MREN, 32 Avenue Foch, F62930, Wimereux - FRANCE.
E-mail: Santer@univ-littoral.fr


## INTRODUCTION

A well-knowledge of the aerosol optical properties (AOPs) is a strong requirement for achieving the atmospheric correction over ocean. AERONET (AErosol RObotic NETwork) provides valuable inputs. They are different approaches in the use of one AERONET data which combines at a given time multi-spectral measurements of the extinction of the solar beam and of the sky radiance fields:

- A direct transformation of the sky radiance into the aerosol phase function (APF) using the WOPAER tool [1].
- The AERONET team proposes a micro-physical description of the aerosols through the retrieval of the standard size distributions of the aerosols associated with the aerosol refractive index [2]. This micro-physical database is available on the AERONET web-site.

This AERONET micro-physical description is used to compute the aerosol phase function at 3 wavelengths (440, 675 and 870 nm). We refer this approach as 'AEROPA'.

The individual sets of inherent optical properties (IOPs) can be used to build an aerosol climatology. This generation of MERIS aerosol models (MAMs) has been completed for the 2 Seas (Northern Sea and East English Channel) and for the region of shore of Venice (Aqua Alta Oceanographic Tower, AAOT). The performance of the atmospheric correction (AC) when using different sets of MAMs has been evaluated in this work. We also discuss about the perspectives for Sentinel-3/OLCI.

## THE AEROSOL OPTICAL PROPERTIES FROM AEROPA

A database of aerosol optical thickness (AOT), single scattering albedo (SSA) and phase function ($P_a$) has been downloaded from the AERONET web-site. For that, we selected the AERONET stations located in the English Channel, the South of Northern Sea (2-Seas) and at AAOT.

| Site | N1 | N2 | Site | N1 | N2 |
|---|---|---|---|---|---|
| Dunkerque | 1096 | 173 | RameHead | 10 | 0 |
| Helgoland | 520 | 44 | De Hague | 528 | 89 |
| Lannion | 37 | 5 | AAOT | 5362 | 837 |
| Oostende | 1468 | 104 | Total | 9021 | 1252 |

*Table 1: Number of sequences per station : N1 for Pa, N2 for SSA.*

The selection of the aerosol model is based on the spectral dependency of the aerosol reflectance in the near-infared (NIR) region.

The dispersion of the aerosol phase function is quite important, here at 865 nm, and for two scattering angles as illustrated in Figure 1. Although it is not possible to describe accurately $P_a$, it is important to evaluate the impact of the poor knowledge of $P_a$ on the water reflectance retrieval. An error bar can be generated through the use of maximum and minimum values of $P_a$ and of the spectral dependence of the AOT. Moreover, we cannot get an accurate value of AOT at 865 nm (AOT865). A validation through AOT requires a significant number of matchups to be valid in mean.

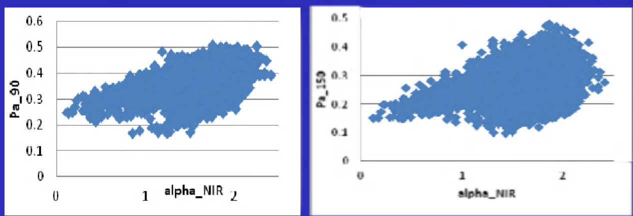


*Fig.1: Aerosol phase function at 870 nm and at two scattering angles for the 3562 sequences.*

## THE STANDARD AEROSOL MODELS FROM AEROPA

We defined 16 classes of IOPs to be in-line with the number of standard aerosol models (SAMs) used in the MERIS ESA Ground Segment (MEGS). The first model is centred at an Angstroem exponent, $\alpha$=0. An increment of $\Delta\alpha$=0.15 with a width of 0.3 have been selected to define each class. Moreover, an iterative filter on $P_a$ has been applied to build classes:

(*i*) At order 0, the mean at the sigma has been computed for the 81 scattering angles and the 3 spectral bands.

(*ii*) In an iterative loop, for the scattering angle ranged within [30°; 150°], sequences for which the relative dispersion is greater than 25 percents were discarded.

| class | center | N | alp_nir | alp_vis | class | center | N | alp_nir | alp_vis |
|---|---|---|---|---|---|---|---|---|---|
| 1 | 0.00 | 2 | 0.12 | 0.22 | 9 | 1.20 | 525 | 1.19 | 1.45 |
| 2 | 0.15 | 9 | 0.20 | 0.33 | 10 | 1.35 | 846 | 1.33 | 1.51 |
| 3 | 0.30 | 42 | 0.36 | 0.56 | 11 | 1.50 | 1253 | 1.47 | 1.56 |
| 4 | 0.45 | 83 | 0.46 | 0.70 | 12 | 1.65 | 1758 | 1.61 | 1.62 |
| 5 | 0.60 | 122 | 0.60 | 0.88 | 13 | 1.80 | 1972 | 1.74 | 1.67 |
| 6 | 0.75 | 171 | 0.74 | 1.08 | 14 | 1.95 | 1401 | 1.86 | 1.74 |
| 7 | 0.90 | 228 | 0.89 | 1.25 | 15 | 2.10 | 554 | 1.98 | 1.83 |
| 8 | 1.05 | 319 | 1.04 | 1.35 | 16 | 2.25 | 119 | 2.10 | 1.93 |

*Table.2: For each of the 16 classes, the nominal centre in $\alpha$, are given the number (N) of sequences per class, the Angstroem exponents between 675 and 870 nm and between 440 and 675 nm.*

The performance of the AC has not to be judged on the retrieval of the AOT but on the possibility to predict the spectral dependence of the aerosol reflectance in the blue region from $\varepsilon$ computed in NIR. More exactly, we extract the aerosol reflectance in the NIR domain, to extrapolate it in the blue region. The quality control is, knowing the spectral dependence of $\varepsilon$ in the NIR, how well do we estimate this spectral dependence in the blue? According to Figure-2, starting from the knowledge of the spectral dependence of $\tau_a P_a$ in the NIR, we get a large dispersion in the prediction of $\tau_a P_a$ in the visible domain.

$$\varepsilon(\lambda,\lambda') = \frac{\log(\rho_a(\lambda)/\rho_a(\lambda'))}{\log(\lambda/\lambda')}$$

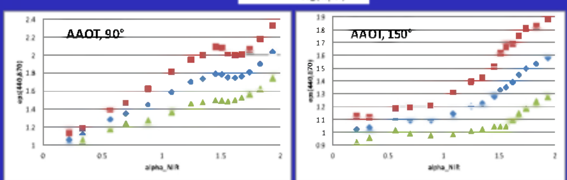


*Fig.2: $\varepsilon$(440,870) for two scattering angles with the mean value (blue diamond), the maximum (red square) and minimum (green triangle) values at one sigma.*

## SEASONAL VARIABILITY

On the AAOT, for the class #12, we did two subsets: winter includes November, December, January, February and March; summer includes May, June, July, August and September. The two sets are comparable: (*i*) in AOT (Table-3); (*ii*) in $P_a$, at least for the two selected scattering angles (Table-4). Within the dispersion, we cannot notice on any of the key aerosol IOPs any seasonal trend. Implicitly, we do not analyze the influence of the relative humidity.

| | lambda | 440 | 670 | 870 | alpha |
|---|---|---|---|---|---|
| Winter | mean | 0.209 | 0.119 | 0.081 | 1.521 |
| 501 | sigma | 0.213 | 0.139 | 0.095 | 0.085 |
| Summer | mean | 0.240 | 0.123 | 0.084 | 1.509 |
| 722 | sigma | 0.199 | 0.124 | 0.085 | 0.086 |

*Table 3: AOT (mean and sigma) in AAOT at 3 wavelengths and a (675,870)*

| | 90 | 120 | 150 | 90 | 120 | 150 | 90 | 120 | 150 |
|---|---|---|---|---|---|---|---|---|---|
| mean | 0.224 | 0.115 | 0.118 | 0.318 | 0.181 | 0.189 | 0.364 | 0.230 | 0.248 |
| sigma | [illegible] | [illegible] | [illegible] | [illegible] | [illegible] | [illegible] | [illegible] | [illegible] | [illegible] |
| percent | 18.4 | 17.2 | 16.6 | 17.3 | 23.3 | 22.7 | 14.9 | 22.6 | 23.4 |
| mean | [illegible] | 0.116 | 0.124 | 0.339 | 0.199 | 0.222 | 0.373 | 0.250 | 0.292 |
| sigma | [illegible] | 0.019 | 0.018 | 0.049 | 0.039 | 0.045 | 0.045 | 0.046 | [illegible] |
| percent | 16.5 | 16.1 | 14.4 | 14.4 | 19.5 | 20.1 | 12.2 | 18.5 | 20.2 |

*Table 4: $P_a$ (mean and sigma) in AAOT at 3 wavelengths and 3 scattering angles: winter (above) and summer (below).*

## SPATIAL HOMOGENEITY

We now consider the two data sets: AAOT and 2-Seas. The similitude between AAOT and the 2-Seas is strong. The AERONET data do not clearly emphasize the need to make nor a seasonal differentiation and neither a geographical differentiation, at least in this case.

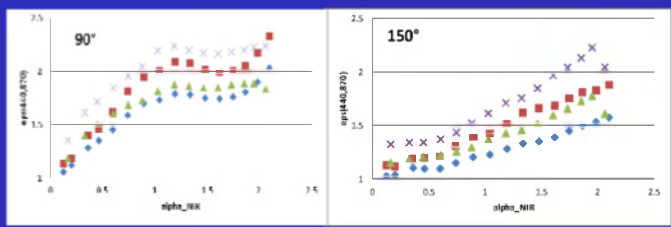


*Fig.3: Comparison of e(440,675) versus a(670,870) with the mean value for AAOT (diamond) and for the 2seas (triangle) and the maximum values for AAOT (square) and for the 2seas (cross).*

## ANALYSIS OF WOPAER DATABASE

The WOPAER database comprises the AOTs and the sky radiances collected to be processed with our APFR (aerosol phase function retrieval) tool. The sky radiance measurements are collected in the principal plane (PPL) or in the almucantar (ALM) geometry at low solar elevation in order to access to the forward scattering region. It is a two step process:

(*i*) Each individual sky radiance sequence is inverted to obtain $P_a$ at 3 wavelengths. Both the PPL and the two ALMs are processed at 870 and 675 nm.

(*ii*) All the inverted $P_a$ are distributed in the 16 classes. Then, all $P_a$ are firstly averaged and then filtered.

The similarity between AEROPA and WOPAER exists on the spectral behaviour of $P_a$ at a scattering angle of 90°. Nevertheless, substantial differences remain in absolute values.

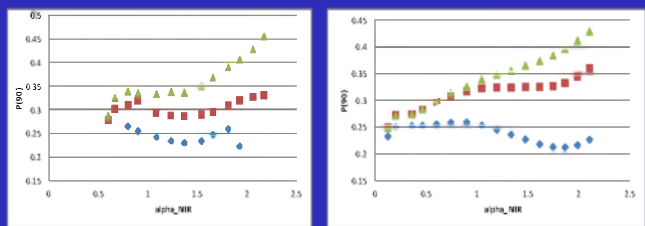


*Fig.4: $P_a$ at AAOT from AEROPA (left plot) and WOPAER (right plot) at 3 wavelengths: 440 nm (diamond), 675 nm (square), 870 nm (triangle).*

## CONCLUSION

We evaluated two different uses of the AERONET data. The natural variability of the aerosol combined to the uncertainty of each method results in substantial errors in the retrieval of $P_a$ or on the spectral dependence of the aerosol reflectance. The dispersion is more pronounced for small aerosols, which make the atmospheric correction more challenging in the coastal areas than in the open ocean. Within the dispersion, the two methods compares quite well as soon as a given class has a representative number of elements.

After the characterization of the aerosol IOPs, it is necessary to build an aerosol climatology in the context of the ADF generation. We did it and used ODESA to evaluate the impact on the L2 MERIS product using MERMAID.

The dispersion of $P_a$ suggests that a validation of the aerosol product restricted to the use of the AOT measurements may be not suitable. The measurement of $P_a$ during matchups is required. This aspect is reported in a companion poster [4].

## References


[1] Santer, R., F. Zagolski, and O. Aznay, 2009. "Aerosol phase function derived from CIMEL measurements", *International Journal of Remote Sensing*, **31** (4), 969-992.

[2] Dubovik, O., and M. D. King, 2000. "A flexible inversion algorithm for retrieval of aerosol optical properties from Sun and sky radiance measurements", *Journal of Geophysical Research*, **105**: 20673–20696.

[3] Zagolski, F., R. Santer, and O. Aznay, 2012. "Apparent optical properties of the aerosols for MERIS/OLCI-S3: Selection of the best LUTs for atmospheric correction over ocean, *Proceedings of MERIS/AATSR & OLCI/SLSTR Preparatory Workshop*, Frascati (Italy), 15-19 October, 2012.

[4] Aznay, O., R. Santer, and F. Zagolski, 2012. "Validation of the MERIS atmospheric correction over ocean using AERONET, *Proceedings of MERIS/AATSR & OLCI/SLSTR Preparatory Workshop*, Frascati (Italy), 15-19 October, 2012



## Acknowledgments

We thanks all the PIs for the AERONET stations we used: G. Zibordi for the AAOT, K. Ruddik for Oostende, and R. Doorfer for the Helgoland, Lannion and Dunkerque. This work was partially supported by the INTERREG 2-Seas program.